HHS Public Access

Author manuscript

Oncogene. Author manuscript; available in PMC 2021 June 09.

Published in final edited form as:

Oncogene. 2021 February ; 40(5): 964–979. doi:10.1038/s41388-020-01539-x.

VEGF-C Mediates Tumor Growth and Metastasis Through Promoting EMT- Epithelial Breast Cancer cell Crosstalk

Deguang Kong[1,2,*], **Hengbo Zhou**[1,3,*], **Deepika Neelakantan**[1,4], **Connor J. Hughes**[1,5,6], **Jessica Y. Hsu**[1,5], **Ramakrishnan Rajaram Srinivasan**[7], **Michael T. Lewis**[7], **Heide L. Ford**[1,3,4,5,6,#]

[1]Department of Pharmacology, University of Colorado Anschutz Medical Campus, Aurora, Colorado, USA

[2]Department of General Surgery, Zhongnan Hospital of Wuhan University, Wuhan, Hubei, China

[3]Program in Cancer Biology, University of Colorado Anschutz Medical Campus

[4]Program in Molecular Biology, University of Colorado Anschutz Medical Campus

[5]Program in Pharmacology, University of Colorado Anschutz Medical Campus

[6]Medical Scientist Training Program, University of Colorado Anschutz Medical Campus

[7]Lester and Sue Smith Breast Center, Baylor College of Medicine, Houston, Texas, USA

Abstract

It is well established that a subset of cells within primary breast cancers can undergo an epithelial to mesenchymal transition (EMT), although the role of EMT in metastasis remains controversial. We previously demonstrated that breast cancer cells that had undergone an oncogenic EMT could increase metastasis of neighboring cancer cells via non-canonical paracrine-mediated activation of GLI activity that is dependent on SIX1 expression in the EMT cancer cells. However, the mechanism by which these SIX1-expressing EMT cells activate GLI signaling remained unclear. In this study, we demonstrate a novel mechanism for activation of GLI-mediated signaling in epithelial breast tumor cells via EMT cell-induced production and secretion of VEGF-C. We show that VEGF-C, secreted by breast cancer cells that have undergone an EMT, promotes paracrine-mediated increases in proliferation, migration and invasion of epithelial breast cancer cells, via non-canonical activation of GLI-signaling. We further show that the aggressive phenotypes, including metastasis, imparted by EMT cells on adjacent epithelial cancer cells can be disrupted by either inhibiting VEGF-C in EMT cells or by knocking down NRP2, a receptor which interacts with VEGF-C, in neighboring epithelial cancer cells. Interrogation of TCGA and GEO public datasets supports the relevance of this pathway in human breast cancer, demonstrating that VEGF-

[#]**Corresponding author:** Heide L. Ford, Ph.D., Department of Pharmacology, University of Colorado Anschutz Medical Campus, Aurora 80045, Colorado, USA. Tel: 303-724-3509, Fax: 303-724-3663, Heide.Ford@cuanschutz.edu.
[*]These authors equally contributed to this work

Conflict of Interest M.T.L is a Founder and Limited Partner in StemMed Ltd, and a Founder and Manager in StemMed Holdings, its General Partner. He is also a Founder and equity stake holder in Tvardi Therapeutics Inc. The remaining authors do not have any conflicts of interest.

C strongly correlates with activation of Hedgehog signaling and EMT in the human disease. Our study suggests that the VEGF-C/NRP2/GLI axis is a novel and conserved paracrine means by which EMT cells enhance metastasis, and provides potential targets for therapeutic intervention in this heterogeneous disease.

Keywords

breast cancer; EMT; VEGF-C; GLI

Introduction:

Aside from skin cancer, breast cancer is the most prevalent malignant disease among women [1]. Despite advancements in screening and therapy, the disease still claims over 600,000 lives per year worldwide, and almost all of these deaths result from metastases [1, 2]. Thus, understanding the mechanisms that mediate breast cancer growth and metastasis is essential for developing effective strategies to combat this malignancy.

It is well accepted that most cancers exhibit significant intratumoral heterogeneity [3–7]. During the course of tumor evolution, different sub-clonal populations of cells arise via the acquisition of mutations or induction of epigenetic alterations that often are stimulated by the tumor microenvironment [8][9]. The genotypic and phenotypic diversity within tumors has a significant impact on clinical treatment, leading to tumor progression and poor outcomes [9–11]. Such heterogeneity can result in incorrect diagnoses or treatment, as well as resistance to chemotherapy, as minor clones can be selected for during the course of the treatment [7, 10].

Intratumoral heterogeneity contributes to tumor progression via numerous mechanisms, including cooperativity between phenotypically different cells within a tumor. For example, Berns and colleagues found that in vivo crosstalk between neuroendocrine and mesenchymal-like small cell lung cancer cells led to enhanced metastatic capacity of the neuroendocrine cells within the tumor [12]. Additionally, Polyak and colleagues demonstrated that a minor cell sub-clone within breast cancers could drive tumor growth via enhancing the proliferation of all cells within the tumor [13]. Our laboratory previously demonstrated that breast cancer cells that underwent an oncogenic epithelial-to-mesenchymal transition (EMT) increased the metastatic capabilities of neighboring epithelial tumor cells via both canonical and non-canonical activation of the GLI transcription factor dependent on SIX1 expression in the EMT cells [14]. However, the mechanism by which EMT cells non-canonically activate GLI signaling, thereby imparting aggressive properties on neighboring tumor cells, remained unclear.

Herein, we describe our novel finding that VEGF-C, which is transcriptionally upregulated by SIX1 in tumor cells that have undergone an EMT, mediates paracrine activation of GLI in epithelial tumor cells via binding to the Neuropilin-2 receptor (NRP2), resulting in enhanced growth and metastases of epithelial cancer cells. We demonstrate that inhibition of the Vegf-c/Nrp2 axis results in diminished crosstalk between the two tumor cell types, inhibiting epithelial tumor cell growth and metastasis. Interrogation of the breast TCGA dataset

underscores the relevance of the VEGF-C/GLI axis in the human disease as both Hedgehog signaling and EMT significantly correlate with VEGF-C expression. Our data suggest that EMT mediated VEGF-C secretion, which was thought to primarily influence lymphangiogenesis in the tumor microenvironment [15, 16], imparts novel and conserved paracrine effects on epithelial cells within the primary tumor, mediating GLI signaling and enhancing metastasis of otherwise less aggressive cells.

Results:

Crosstalk in a spontaneous model of EMT/epithelial cancer cells.

We previously induced EMT in HMLER and MCF7 breast cancer cells via overexpression of EMT associated transcription factors (aTF) [14], and then examined crosstalk between the HMLER-TWIST/SNAIL or the MCF7-SIX1 cells with their control epithelial counterparts. Because these models all use overexpression of EMT aTFs to induce EMT, we attempted to identify spontaneous models of EMT/epithelial breast cancer cells, in which EMT-aTFs are not ectopically expressed for additional studies. To this end, we characterized the Met1 and DB7 models of mammary carcinoma. The Met1 line was previously characterized to have higher metastatic potential than the DB7 line, and was derived from a mammary carcinoma that arose in an FVB/N-Tg (MMTV-PyVmT) mouse [17]. DB7 cells were shown to be less motile and metastatic than Met1 cells, and were derived from a mammary tumor that arose in an FVB/N-Tg (MMTV-PyVmTY$^{315F/Y322F}$) mouse [17]. Because of the differences in metastatic nature of these two closely related lines, we asked whether their EMT characteristics differed.

Using qRT-PCR, western blot analysis, and immunocytochemistry (ICC), we compared the expression levels of Six1 and markers associated with EMT (E-cadherin, N-cadherin and Vimentin). Met1 cells expressed higher levels of Six1, as well as N-cadherin and Vimentin (Supplementary Fig. 1A–E), when compared to DB7 cells, suggesting that these cells have undergone at least a partial EMT. In contrast, DB7 cells expressed more Cdh1/E-cadherin than Met1 cells (Supplementary Fig. 1C–D). As anticipated, we confirmed that Met1 cells were more migratory and invasive than DB7 cells (Supplementary Fig. 1F–I). Together, these data suggest that Met1 cells exhibit significantly more EMT characteristics than DB7 cells.

Six1 expression in EMT cells (Met1) is required for paracrine-mediated increased aggressiveness of epithelial carcinoma cells (DB7).

Our previous studies showed that Six1 could induce an EMT in certain contexts [18–20], and that either on its own, or downstream of TWIST1 and SNAIL1, its expression was required to enhance the aggressive characteristics of epithelial tumor cells in a paracrine manner [14]. To examine whether this same mechanism is in play in cells in which EMT aTFs have not been ectopically overexpressed, we transferred conditioned medium (CM) from the more EMT-like, Met1 cells, to the more epithelial, DB7, mammary carcinoma cells. As was observed in the HMLER-Ctrl/HMLER-TWIST1/SNAIL1 CM experiments described previously [14], DB7 cells cultured in Met1 CM did not exhibit an alteration in their EMT marker profile (E-cadherin and N-cadherin) (Supplementary Fig. 2A). However,

proliferation of DB7 cells was moderately, but significantly increased when the cells were cultured in Met1 CM, but not when cultured in Met1 CM collected from cells in which Six1 was KD (Supplementary Fig. 2B, C). Importantly, despite no change in EMT marker expression, migration and invasion of DB7 cells was enhanced when the cells were cultured in Met1 CM (Supplementary Fig. 2D–G). Furthermore, treatment of DB7 cells with CM collected from Met1 cells in which Six1 was knocked down (Supplementary Fig. 2B), led to an abrogation of Met1 CM-induced migration, and invasion of DB7 cells (Supplementary Fig. 2D–G). Thus, these data demonstrate that Six1 is critical to mediate EMT/epithelial tumor cell crosstalk, even in models where EMT spontaneously arises and is not artificially induced.

Expression of Six1 in Met1 cells enhances the aggressiveness of DB7 cells via paracrine activation of Gli signaling.

We previously demonstrated, in models induced to undergo an EMT via ectopic expression of TWIST1, SNAIL1 or SIX1 TFs, that CM from EMT cells led to GLI activation in the epithelial tumor cells in a manner that was dependent on SIX1 EMT cell expression [14]. Further, we demonstrated that activation of GLI in the epithelial tumor cells was required to mediate the increase in migration and invasion observed in response to EMT CM treatment. To test whether this mechanism is conserved in a spontaneous model of EMT/epithelial tumor cell crosstalk, we first asked whether Gli signaling was activated in DB7 cells in response to treatment with Met1 CM using Gli1 and Patched1 mRNA as readouts of activation of the pathway [14]. Increased expression of Gli1 and Ptch1 mRNA was observed in DB7 cells cultured in Met1 CM when compared to their own CM or in CM from Met1 cells with Six1 KD (Supplementary Fig. 3A and B). Additionally, treatment of DB7 cells with a GLI inhibitor, GANT61, abolished the ability of Met1 CM to enhance the proliferation, migration and invasion of DB7 cells (Supplementary Fig. 3C–G).

Increased VEGF-C in the CM of EMT cells promotes aggressive properties in epithelial tumor cells via GL1 activation.

Since we observed paracrine increases in response to EMT cell CM, we reasoned that there are soluble factors in the CM that can activate GLI signaling. Given that GLI is canonically activated downstream of Hedgehog (Hh) signaling, Hh ligands could be responsible for paracrine activation of GLI in epithelial tumor cells in response to CM from EMT cells. In mammals, three secreted Hh ligands, Sonic Hedgehog (SHH), Indian Hedgehog (IHH) and Desert Hedgehog (DHH) bind to Patched-1 (PTCH 1) or Patched-2 (PTCH 2) receptors, relieving the inhibition by Patched on Smoothened (SMO), resulting in activation of canonical GLI-mediated signaling [21]. In addition to canonical activation of GLI, non-canonical activation of GLI independent of the HH-PTCH-SMO axis has been shown to occur in many different kinds of cancers [22, 23]. Our previous data demonstrated that paracrine activation of GLI in response to EMT/epithelial breast cancer cell crosstalk can occur by canonical or non-canonical mechanisms, dependent on the model system used [14]. In line with this finding, we did not observe an increase in any of the known Hedgehog (Hh) ligands (Shh, Ihh, or Dhh) within the CM of Met1 (EMT) cells when compared to that of epithelial DB7 mammary carcinoma cells (Supplementary Fig.4), suggesting that a non-canonical mechanism of Gli activation is at play in this system as well. Thus, additional

soluble factors are secreted by EMT cells to regulate Gli signaling in epithelial carcinoma cells, increasing the aggressive characteristics of the epithelial carcinoma cells, often without inducing an associated EMT.

We previously showed that SIX1 transcriptionally upregulates VEGF-C in breast cancer cells, leading to enhanced lymphangiogenesis and metastasis [24, 25]. Because we demonstrated a critical role for SIX1 in paracrine activation of GLI in both the spontaneous and induced models of EMT, we asked whether VEGF-C may be capable of regulating GLI in epithelial tumor cells and thereby mediate the induction of aggressive phenotypes in those cells. To this end, we used all three models in which SIX1 was shown to activate GLI in a paracrine manner: MCF7-Ctrl/MCF-SIX1 [14], HMLER-Ctrl/HMLER-SNAIL1 [14], and DB7/Met1 (shown here). In HMLER and DB7/Met1models, SIX1 KDs were performed with siRNA, which, on average, achieved an approximately 70% KD (Supplementary Fig. 2B and Supplementary Fig. 5). We found that VEGF-C mRNA and protein (as measured by western blot in the cell lysate or by ELISA in the cell lysate or CM) is upregulated by SIX1 in all three EMT cell line models (Fig. 1), uncovering a conserved mechanism of VEGF-C regulation in cells that have undergone an EMT via different means.

To test whether VEGF-C secretion, downstream of SIX1, results in non-canonical activation of GLI, we treated the epithelial breast cancer cells with their own CM or with EMT cell CM, in the presence or absence of a VEGF-C neutralizing antibody, and then measured GLI activation in the treated cells using a 7xGLI-GFP reporter [14]. GLI signaling is activated when MCF7-Ctrl cells are treated with MCF7-SIX1 CM. However, neutralization of VEGF-C (using the SC-374628 antibody) in the MCF7-SIX1 CM abrogates this increased GLI activity (Fig. 2A). This result was also observed in the HMLER-Ctrl/HMLER-SNAIL1 and DB7/Met1 systems (Fig. 2B and C).

In order to exclude potential non-specific effects of the neutralizing antibody, we used a second VEGF-C neutralizing antibody (SAB1411757), as well as siRNA to KD VEGF-C in EMT cells after which we collected CM to be used on the epithelial carcinoma cells transfected with the 7xGLI-GFP reporter. About a 70% VEGF-C KD was achieved using siRNA (Supplementary Fig 6). As seen in Fig. 2D–F, KD of VEGF-C in MCF7-SIX1, HMLER-SNAIL1, or Met1 cells significantly decreased the paracrine-mediated activation of GLI in the epithelial carcinoma Ctrl cells, as did addition of a different VEGF-C antibody than that used in the first experiment (Supplementary Fig.7). Furthermore, addition of recombinant human (rh) VEGF-C into CM collected from HMLER-SNAIL1 SIX1 KD cells or recombinant mouse (rm)-Vegf-c into CM from Met1 Six1 KD cells (in which VEGF-C levels are reduced), rescued GLI activation in the epithelial tumor cells cultured in the VEGF-C supplemented CM (Fig. 2G and H). Taken together, VEGF-C can clearly activate GLI signaling in numerous contexts.

Because VEGF-C belongs to a family of secreted ligands, and recent studies have implicated two other VEGF ligands (VEGF-A and VEGF-D) in Hh pathway activation [23, 26], we asked whether VEGF-C activation of GLI was unique to EMT/epithelial carcinoma cell crosstalk. To this end, we first directly added the three ligands, VEGF-C, A, or D, to MCF7 epithelial breast cancer cells and interrogated GLI activation using the 7xGLI-GFP reporter.

Surprisingly, we found that only VEGF-C was able to activate the reporter in this setting (Supplementary Fig. 8). These data suggest that VEGF-C secreted by EMT cells can uniquely activate GLI signaling in epithelial cancer cells in these contexts.

Inhibition of VEGF-C in EMT breast cancer cells suppresses paracrine induction of aggressive phenotypes imparted on epithelial cancer cells.

To test whether VEGF-C in the CM from EMT cells is responsible for the observed phenotypes, EMT marker expression, migration, invasion and proliferation were examined in epithelial tumor cells after treatment with EMT CM +/− VEGF-C neutralizing antibody (Ab). In all three systems tested, epithelial tumor cells cultured in EMT cell CM grew faster than when cultured in their own CM, and addition of the VEGF-C neutralizing Ab (SC-374628) in EMT cell CM inhibited the observed increases in proliferation (Fig. 3A–C). Further, neutralization of VEGF-C in MCF7-SIX1 CM restored expression of membranous E-Cad in MCF7-Ctrl cells cultured in MCF7-SIX1 CM (Fig. 4A and B), a system where EMT markers were previously shown to change in the epithelial tumor cells in response to the EMT CM [14]. In the HMLER-Ctrl/HMLER-SNAIL1 and DB7/Met1 systems, blocking VEGF-C inhibited the increase in migration (Fig. 4C–F) and invasion (Fig. 4G–J) observed in Ctrl epithelial tumor cells receiving EMT cell CM.

To determine whether the EMT/epithelial cancer cell crosstalk has consequences in vivo, and whether VEGF-C production by EMT cells is critical for such crosstalk, we mixed luciferase tagged DB7 epithelial mammary carcinoma cells with Met1-scramble (SCR) and Met1-shVegf-c cells (at a 4:1 ratio of epithelial: EMT cancer cells) and injected the mixed cells into the 4th mammary fat pad of FVB mice. Luciferase signal (which tracks specifically the epithelial DB7 cells) was monitored over time, and total tumor volume was measured using calipers (which tracks the epithelial and EMT cancer cell growth together). After 4 weeks, the tumors were surgically removed to enable examination of metastasis over time. Metastasis of the epithelial cancer cells was then tracked weekly via IVIS imaging. As Supplementary Fig. 9 shows, the DB7 epithelial mammary carcinoma cells grew faster when they were mixed with the Met1 EMT cells as compared to when they were mixed with DB7 non-tagged cells. Importantly, KD of Vegf-c in the Met1 cells abolished the effects of Met1 cells on DB7 cell growth. Though these cells were previously shown to metastasize in FVB mice [17], we did not observed sufficient metastases in this setting to draw any clear conclusions regarding metastatic dissemination. Nonetheless, these data demonstrate that inhibition of Vegf-c in the EMT cells is an effective means to inhibit paracrine-mediated induction of growth of epithelial mammary carcinoma cells within a heterogeneous tumor.

Neuropilin-2 Receptor (NRP2) expression on epithelial cancer cells is required to mediate the paracrine effects of VEGF-C from EMT cells.

NRP2 has been shown to bind to VEGF-C and activate a VEGF-C-NRP2 signaling axis in both lymphatic endothelial cells and in tumor cells, including breast cancer [16, 27]. To determine whether NRP2, when expressed on the surface of epithelial cancer cells, is the receptor through which VEGF-C activates GLI and enhances proliferation, migration, and invasion of these cells, we knocked down NRP2 in the epithelial breast cancer cells, which was confirmed by flow cytometry to examine surface levels of NRP2 (Supplementary Fig.

10A–F) and then cultured the cells in their own CM or CM from EMT cells +/− a neutralizing VEGF-C antibody. We found that neutralizing VEGF-C in MCF7-SIX1 CM or knocking down NRP2 in MCF7-Ctrl cells abolished the MCF7-SIX1 CM-mediated increase of GLI1 mRNA (Fig. 5A) and 7xGLI -GFP reporter activity (Fig. 5B) in MCF7-Ctrl cells. Similar results were seen in both the HMLER-Ctrl/HMLER-SNAIL1 and the DB7/Met1 cell lines, demonstrating that this mechanism is at play in multiple contexts (Fig. 5C–F).

Both NRP2 and FLT4 (VEGFR3) are required for EMT/epithelial tumor cell crosstalk.

NRP2 interacts with FLT-4 (VEGFR3) to mediate lymphatic vessel sprouting [28]. Thus, as anticipated, KD of FLT-4 in MCF7-Ctrl cells, or use of an antibody that targets FLT-4 in those cells, phenocopies KD of NRP2 in MCF7-Ctrl cells when treated with MCF7-SIX1 cell CM, inhibiting GLI activation (Supplementary Fig. 7 and 11A). Further, FLT-4 KD recapitulates the phenotype observed when a VEGF-C blocking antibody is added to the MCF7-SIX1 CM, which also disrupts activation of GLI signaling in MCF7-Ctrl cells in response to treatment with MCF7-SIX1 CM (Supplementary Fig. 11A).

To demonstrate that signaling is activated downstream of FLT-4/NRP2, we measured downstream effectors, AKT and ERK, which are known to be phosphorylated upon activation of FLT-4 [29]. Indeed, p-AKT and p-ERK levels increased in MCF7-Ctrl cells treated with MCF7-SIX1 CM (Supplementary Fig. 11B Left). Similar activation of Akt and Erk was observed in the DB7/Met1 system, where addition of Met1 CM enhanced p-Akt and p-Erk levels in DB7 cells (Supplementary Fig. 11B Right).

Inhibition of the Vegf-c-Nrp2 axis suppresses paracrine-mediated tumor growth and metastasis in *vivo*.

To determine whether the Vegf-c-Nrp2 axis imparts aggressive properties on epithelial cancer cells in *vivo*, we knocked down Nrp2 in DB7 cells (Supplementary Fig. 10E and F) and knocked down Vegf-c in Met1 cells (Supplementary Fig. 12A and B). Following the creation of KD lines, we tagged the DB7-SCR and DB7-shNRP2 cells with luciferase (Supplementary Fig. 12C), after which we mixed the tagged DB7s with non-tagged DB7 or Met1 cells (at a 4:1 ratio of epithelial cancer:EMT cells) and injected the mixed cells into the 4^{th} mammary fat pad of nude mice, since we did not observe overt metastasis in vivo when these cells were injected into FVB mice. Tumor growth and metastasis were measured over time using calipers (which measures total tumor volume) and IVIS imaging (which measures the epithelial cancer cells specifically). After three weeks, we removed the primary tumors and continued to monitor the mice for metastasis. As shown in Fig. 6A and B, DB7 cells grew faster when they were mixed with Met1 cells as compared to when they were mixed with DB7 non-tagged cells. However, when Nrp2 was KD in DB7-Luc cells, or when Vegf-c was KD in Met1 cells, the enhanced growth of DB7 cells was abolished (Fig. 6A and B). This alteration in growth of DB7 cells at the primary tumor site also translated into smaller overall tumor size via caliper measurements (Fig. 6C). In order to exclude the effect of Nrp2 KD and Vegf-c KD on proliferation of the cells themselves, we performed proliferation assays using DB7-SCR and DB7-shNrp2 cells, or Met1-SCR and Met1-shVegf-c cells in vitro. As seen in Supplementary Fig. 13A and B, neither Nrp2 nor Vegf-c KD suppresses the growth of these cancer cells in which the KD has been performed in vitro. We

additionally injected the DB7-Nrp2 KD and control cells into the mammary fat pads of immunocompromised mice, and did not observe decreased growth in the DB7-Nrp2 KD cells themselves (Supplementary Fig. 13C). Thus, loss of Nrp2 decreases growth of DB7 cells via a mechanism that requires crosstalk with the Met1 cells both in vitro and in vivo.

Finally, we assessed the role of the Vegf-c/Nrp2 axis on metastasis mediated through tumor cell crosstalk. Importantly, the epithelial DB7 cells metastasized more efficiently when co-injected with Met1 cells, and KD of Vegf-c in the Met1 (EMT) cells, or KD of Nrp2 in DB7 (epithelial carcinoma) cells, abolished this effect (Fig. 6D). Taken together, these data clearly demonstrate that crosstalk between EMT and epithelial cancer cells can promote proliferation *and* metastasis in heterogeneous breast cancers, and that inhibition of the Vegf-c-Nrp2-Gli axis can disrupt the crosstalk specifically between the tumor cells.

GLI signaling pathway genes significantly correlate with VEGF-C in human breast tumors.

To determine, using a rigorous and unbiased method, whether VEGF-C may activate Hh signaling and correlate with EMT in human breast cancer, we analyzed the PanCancer Atlas TCGA breast cancer dataset to identify genes significantly correlated with VEGF-C expression. Upon performing gene-by-gene Pearson correlations with VEGF-C expression and submitting ranked correlation coefficients to GSEA pathway analysis, we found that VEGF-C levels are significantly correlated with both Hedgehog signaling and EMT in human breast cancer (Fig. 7A and B). We then more specifically examined correlations between all the VEGF ligands and components of the Hh signaling pathway. As can be seen in Fig. 7 C, a statistically significant correlation of VEGF-C and genes that are transcriptionally activated downstream of Hh signaling (GLI1, GLI2 and PTCH2) can be observed. Intriguingly, in contrast to VEGF-A and VEGF-B, VEGF-D shared similar correlations as VEGF-C, suggesting that in the human setting, VEGF-C and D may have redundant functions in activating this pathway despite us not observing an effect with VEGF-D in our model systems. Nonetheless, these results strongly suggest that VEGF-C can indeed contribute to activation of GLI signaling in human breast cancer.

Discussion

Epithelial to mesenchymal transition (EMT) is a highly dynamic cellular program involved in embryonic development, wound healing, and tumorigenesis [30]. In breast and other cancers, EMT results in altered adhesion and cell polarity, as well as increased motility and invasion [31]. However, recent studies have suggested that EMT is not required for metastasis in mouse mammary carcinoma models [32], as well as in a mouse model of pancreatic cancer [33]. However, neither study examined the potential effect of crosstalk between EMT and non-EMT as a contributor to metastatic disease.

SIX1 is an EMT-aTF [34], and its aberrant activation has been implicated in the progression of numerous malignancies, including breast cancer [20, 35, 36]. In breast cancer, SIX1 can autonomously promote proliferation [37], migration [18] and EMT [34]. In addition to these tumor cell autonomous effects, SIX1 also promotes breast cancer progression via non-cell autonomous means, where high SIX1 expressing breast cancer cells (that have undergone an EMT) can increase the aggressive properties of neighboring epithelial tumor cells. However,

an understanding of the precise mechanism by which SIX1 non-cell autonomously mediates metastasis remained unknown.

Previous studies demonstrated that SIX1 transcriptionally upregulates VEGF-C, resulting in lymphangiogenesis and increased metastasis [24]. Herein, we demonstrate that VEGF-C expression/secretion mediated by SIX1 in EMT cells is also critical to mediate crosstalk between EMT and epithelial breast cancer cells in a heterogeneous tumor. We show that SIX1-expressing EMT cells activate GLI signaling in epithelial cancer cells via increased production of VEGF-C, and that the VEGF-C/GLI axis promotes proliferation, migration, and invasion of epithelial cancer cells. Most importantly, we show that this crosstalk is relevant to tumor growth and metastasis in vivo, and perhaps provides an explanation for why fate mapping experiments, in which EMT cells were said to not enhance metastasis [32], may have not completely assessed the effects of EMT in tumors. Finally, we show that VEGF-C significantly positively correlates with both EMT and GLI signaling in human breast cancer (Fig. 7).

VEGF-C was identified as a ligand for VEGFR-2 and VEGFR-3, and plays an important role in lymphangiogenesis and angiogenesis during embryonic development [38, 39]. In addition, VEGF-C promotes tumor-associated lymphangiogenesis, angiogenesis [15, 24, 40], immune tolerance [41], tumor cell proliferation, and migration and invasion [42–44]. Our data demonstrate a novel role for VEGF-C in mediating tumor progression. We show that VEGF-C is the key mediator through which SIX1 non-canonically activates GLI signaling to enhance tumor progression (growth and metastasis) of cells that would otherwise not be aggressive within a tumor. These data add suggest that targeting VEGF-C may have numerous anti-tumor effects. VGX-100, the human monoclonal antibody against VEGF-C, has been tested in preclinical trails in acute myeloid leukemia, and can suppress tumor progression by inducing cellular differentiation in *vivo* [45]. Recently, several studies showed sVEGFR3-Fc, a soluble VEGF-C competitor, reduces tumor proliferation and metastasis [46, 47]. Together, these data suggest that targeting VEGF-C may be a viable therapeutic option.

VEGF-C exerts its action by binding to receptors to transduce extracellular stimuli into intracellular signals. FLT4/VEGFR3 is a well-known receptor of VEGF-C. VEGF-C also binds to the NRP family of receptors including NRP1 and NRP2, with preferential binding to NRP2 [48]. Intriguingly, NRPs have recently been linked to GLI signaling [23, 26, 49]. In triple-negative breast cancer (TNBC), a VEGF-A/NRP2 axis was shown to activate GLI1 signaling in an autocrine manner [26]. In lung adenocarcinoma cells, HH/GLI signaling is upregulated by stromal VEGF-A mediated stimulation of NRP2 [23]. Herein, we describe a similar role for VEGF-C. Compared to other VEGF family members, VEGF-C shares the highest percent identity with VEGF-A (about 30%) [38], and thus VEGF-C may activate GLI signaling through binding to NRP2 via a conserved region between the two VEGF proteins. However, we surprisingly found that at least in the models tested, VEGF-C, but not VEGF-A or D, is the mediator of GLI activation. We cannot rule out a role for additional ligands in GLI activation in the tumor cells or in the tumor microenvironment. It is possible that the EMT aTFs act primarily through VEGF-C, but that other mechanisms at play in the tumor itself or in the tumor microenvironment may activate VEGF-D (or other VEGF family

members) which in particular contexts can also activate GLI signaling. Furthermore, because we show that NRP2 likely acts with VEGFR3/FLT4 (Fig. 8), these data also suggest that more than one VEGF ligand may influence this pathway in an in vivo context. Several studies have shown an important role for the interaction between NRP2 and FLT4 in lymphatic vessel sprouting [28, 50]. Our study suggests that similarly, the two receptors may act together to mediate VEGF-C action on epithelial tumor cells, resulting in GLI activation.

Aberrant HH/GLI signaling is observed in many tumors, and the HH pathway has therefore been identified as a promising therapeutic target. Vismodegib and Sonidegib, 2 different inhibitors of SMO, while efficacious in basal cell carcinoma, where activating mutations of the canonical pathway are found, have produced disappointing results in several solid tumors [51–53]. Non-canonical HH–GLI signaling is independent of SMO, and thus such activation of GLI signaling may explain the failure of SMO antagonists in these cancers. Prospective molecular profiling of heterogeneous breast cancers to assess their VEGF-C expression might be used to identify patients likely to benefit from VEGF-C-NRP2/FLT4 axis blockade, with or without conventional chemotherapy or other promising biological approaches.

Methods:

Cell culture.

MCF7 derivative cell lines were described previously [14]. The cell lines were profiled via short tandem repeat (STR) profiling at the beginning (April 2015) and end (October 2019) of this study. HMLER cell lines were a generous gift from the Weinberg Lab, and are not included in ATCC or DSMZ. DB7 and Met1 cells were a generous gift from Dr. Jennifer Richer (University of Colorado Anschutz Medical Campus, Aurora, CO) with permission granted by Alexander Borowsky (University of California, Davis, CA). Details describing all drug or siRNA treatments of cells are included in the supplemental methods, while shRNA sequences are listed in Supplementary Table 1.

Quantitative real-time PCR (RT-qPCR).

RNA was prepared using the Direct-zol™ RNA MiniPrep Kit (Zymo Research, R2051). cDNA was reverse transcribed from 1 μg total RNA using the iScript cDNA Synthesis Kit (BioRad, 1708890). RT-qPCR was performed with the ssoFast Evagreen supermix (BioRad, 1725201). Sequences of primers are listed in Supplementary Table 2.

Western blot analysis.

Equal amounts of lysates (30–50ug) were electrophoresed and transferred onto polyvinylidene difluoride (PVDF) membranes. The membranes were subsequently blocked in 5% milk in TBST, and probed with primary antibodies at 4°C overnight. Antibodies are listed in Supplementary Table 3.

ELISA and Immunocytochemistry.

(ICC) The VEGF-C (MyBioSource, MBS2600109), Shh (R & D systems, MSHH00), Ihh (Abclonal, RK02929) and Dhh (Aviva, OKEH03264) levels in the conditioned media were

measured using ELISA, according to manufacturer's instructions. Conditions of ICC can be found in the Supplemental Methods.

GLI reporter assays.

GLI reporter assays were performed as previously described [14]. Details can be found in Supplemental Methods.

Cell proliferation assays.

For CellTiter-Glo assays, 1500 cells incubated with various CMs were plated in 96-well plates. Day 0 time point was measured 6h post plating. Following 24-, 48-, 72- or 96-hours of incubation, day1–4 time points were analyzed. 100 μl of CellTiter-Glo® Reagent (Promega Corporation, G9241) was added to each well and incubated at room temperature for 30 mins and luminescence was measured. Incucyte assays are described in detail in the supplemental methods.

Migration and invasion assays.

Cell migration and invasion assays were performed as previously described [14].

Flow cytometry assays for NRP2.

Cells were harvested and stained with human/mouse Neuropilin-2 APC-conjugated antibody (R&D, FAB22151A) according to the manufacturer's instructions. The NRP2 level on the surface was detected using flow cytometry.

In Vivo Experiments.

Five to 6-week-old female athymic NCr-nu/nu and FVB mice were purchased from Charles River Labs and maintained under Specific Pathogen-Free (SPF) conditions. All animal protocols were reviewed and approved by the Institutional Animal Care and Use Committee at University of Colorado Anschutz Medical Campus. Specific details about the individual animal experiments can be found in the supplemental methods.

Pairwise gene correlation using TCGA BRCA dataset

Degree of relationship between VEGFC expression and all other genes was performed by calculating a Pearson correlation coefficient between z-score converted VEGFC expression and gene *y* for all genes mapped in the TCGA BRCA data set. Pearson correlation coefficients for all genes were subsequently ranked, and GSEA was performed on the ranked list of genes using the MSigDB Hallmarks gene set collection..

Statistical analysis.

Statistical analyses for all studies are outlined in the supplemental methods.

Supplementary Material

Refer to Web version on PubMed Central for supplementary material.

Acknowledgements

This work was supported by R01CA224867 to HLF and MTL, and F99CA234940 to HZ. We would like to thank the Functional Genomics Shared Resource (SR), the Cell Technologies SR, and the Animal Imaging SR of the University of Colorado Cancer Center (P30CA046934) for help with these studies. We would also like to acknowledge support from The Dan L. Duncan Comprehensive Cancer Center (BCM, P30CA125123) and the Cancer Prevention and Research Initiative of Texas (CPRIT) (BCM, RP170691).

References

1. Bray F, Ferlay J, Soerjomataram I, Siegel RL, Torre LA, Jemal A. Global cancer statistics 2018: GLOBOCAN estimates of incidence and mortality worldwide for 36 cancers in 185 countries. CA Cancer J Clin 2018; 68: 394–424. [PubMed: 30207593]
2. Valastyan S, Weinberg RA. Tumor metastasis: molecular insights and evolving paradigms. Cell 2011; 147: 275–292. [PubMed: 22000009]
3. Aparicio S, Caldas C. The implications of clonal genome evolution for cancer medicine. N Engl J Med 2013; 368: 842–851. [PubMed: 23445095]
4. Gerlinger M, Rowan AJ, Horswell S, Math M, Larkin J, Endesfelder D et al. Intratumor heterogeneity and branched evolution revealed by multiregion sequencing. N Engl J Med 2012; 366: 883–892. [PubMed: 22397650]
5. Lindstrom LS, Yau C, Czene K, Thompson CK, Hoadley KA, Van't Veer LJ et al. Intratumor Heterogeneity of the Estrogen Receptor and the Long-term Risk of Fatal Breast Cancer. J Natl Cancer Inst 2018; 110: 726–733. [PubMed: 29361175]
6. Yang F, Cao L, Sun Z, Jin J, Fang H, Zhang W et al. Evaluation of Breast Cancer Stem Cells and Intratumor Stemness Heterogeneity in Triple-negative Breast Cancer as Prognostic Factors. Int J Biol Sci 2016; 12: 1568–1577. [PubMed: 27994520]
7. Yang F, Wang Y, Li Q, Cao L, Sun Z, Jin J et al. Intratumor heterogeneity predicts metastasis of triple-negative breast cancer. Carcinogenesis 2017; 38: 900–909. [PubMed: 28911002]
8. Burrell RA, McGranahan N, Bartek J, Swanton C. The causes and consequences of genetic heterogeneity in cancer evolution. Nature 2013; 501: 338–345. [PubMed: 24048066]
9. Lin L, Lin DC. Biological Significance of Tumor Heterogeneity in Esophageal Squamous Cell Carcinoma. Cancers (Basel) 2019; 11.
10. McGranahan N, Swanton C. Biological and therapeutic impact of intratumor heterogeneity in cancer evolution. Cancer Cell 2015; 27: 15–26. [PubMed: 25584892]
11. Ma F, Guan Y, Yi Z, Chang L, Li Q, Chen S et al. Assessing tumor heterogeneity using ctDNA to predict and monitor therapeutic response in metastatic breast cancer. Int J Cancer 2020; 146: 1359–1368. [PubMed: 31241775]
12. Calbo J, van Montfort E, Proost N, van Drunen E, Beverloo HB, Meuwissen R et al. A functional role for tumor cell heterogeneity in a mouse model of small cell lung cancer. Cancer Cell 2011; 19: 244–256. [PubMed: 21316603]
13. Marusyk A, Tabassum DP, Altrock PM, Almendro V, Michor F, Polyak K. Non-cell-autonomous driving of tumour growth supports sub-clonal heterogeneity. Nature 2014; 514: 54–58. [PubMed: 25079331]
14. Neelakantan D, Zhou H, Oliphant MUJ, Zhang X, Simon LM, Henke DM et al. EMT cells increase breast cancer metastasis via paracrine GLI activation in neighbouring tumour cells. Nat Commun 2017; 8: 15773. [PubMed: 28604738]
15. Chen JC, Chang YW, Hong CC, Yu YH, Su JL. The role of the VEGF-C/VEGFRs axis in tumor progression and therapy. Int J Mol Sci 2012; 14: 88–107. [PubMed: 23344023]
16. Wang CA, Harrell JC, Iwanaga R, Jedlicka P, Ford HL. Vascular endothelial growth factor C promotes breast cancer progression via a novel antioxidant mechanism that involves regulation of superoxide dismutase 3. Breast Cancer Res 2014; 16: 462. [PubMed: 25358638]
17. Borowsky AD, Namba R, Young LJ, Hunter KW, Hodgson JG, Tepper CG et al. Syngeneic mouse mammary carcinoma cell lines: two closely related cell lines with divergent metastatic behavior. Clin Exp Metastasis 2005; 22: 47–59. [PubMed: 16132578]

18. Micalizzi DS, Wang CA, Farabaugh SM, Schiemann WP, Ford HL. Homeoprotein Six1 increases TGF-beta type I receptor and converts TGF-beta signaling from suppressive to supportive for tumor growth. Cancer Res 2010; 70: 10371–10380. [PubMed: 21056993]
19. Blevins MA, Towers CG, Patrick AN, Zhao R, Ford HL. The SIX1-EYA transcriptional complex as a therapeutic target in cancer. Expert Opin Ther Targets 2015; 19: 213–225. [PubMed: 25555392]
20. Kong D, Liu Y, Liu Q, Han N, Zhang C, Pestell RG et al. The retinal determination gene network: from developmental regulator to cancer therapeutic target. Oncotarget 2016; 7: 50755–50765. [PubMed: 27203207]
21. Varjosalo M, Taipale J. Hedgehog: functions and mechanisms. Genes Dev 2008; 22: 2454–2472. [PubMed: 18794343]
22. Pietrobono S, Gagliardi S, Stecca B. Non-canonical Hedgehog Signaling Pathway in Cancer: Activation of GLI Transcription Factors Beyond Smoothened. Front Genet 2019; 10: 556. [PubMed: 31244888]
23. Po A, Silvano M, Miele E, Capalbo C, Eramo A, Salvati V et al. Noncanonical GLI1 signaling promotes stemness features and in vivo growth in lung adenocarcinoma. Oncogene 2017; 36: 4641–4652. [PubMed: 28368412]
24. Wang CA, Jedlicka P, Patrick AN, Micalizzi DS, Lemmer KC, Deitsch E et al. SIX1 induces lymphangiogenesis and metastasis via upregulation of VEGF-C in mouse models of breast cancer. J Clin Invest 2012; 122: 1895–1906. [PubMed: 22466647]
25. Liu D, Li L, Zhang XX, Wan DY, Xi BX, Hu Z et al. SIX1 promotes tumor lymphangiogenesis by coordinating TGFbeta signals that increase expression of VEGF-C. Cancer Res 2014; 74: 5597–5607. [PubMed: 25142796]
26. Goel HL, Pursell B, Chang C, Shaw LM, Mao J, Simin K et al. GLI1 regulates a novel neuropilin-2/alpha6beta1 integrin based autocrine pathway that contributes to breast cancer initiation. EMBO Mol Med 2013; 5: 488–508. [PubMed: 23436775]
27. Wang J, Huang Y, Zhang J, Xing B, Xuan W, Wang H et al. NRP-2 in tumor lymphangiogenesis and lymphatic metastasis. Cancer Lett 2018; 418: 176–184. [PubMed: 29339213]
28. Xu Y, Yuan L, Mak J, Pardanaud L, Caunt M, Kasman I et al. Neuropilin-2 mediates VEGF-C-induced lymphatic sprouting together with VEGFR3. J Cell Biol 2010; 188: 115–130. [PubMed: 20065093]
29. Makinen T, Veikkola T, Mustjoki S, Karpanen T, Catimel B, Nice EC et al. Isolated lymphatic endothelial cells transduce growth, survival and migratory signals via the VEGF-C/D receptor VEGFR-3. EMBO J 2001; 20: 4762–4773. [PubMed: 11532940]
30. Kalluri R, Weinberg RA. The basics of epithelial-mesenchymal transition. J Clin Invest 2009; 119: 1420–1428. [PubMed: 19487818]
31. Drasin DJ, Robin TP, Ford HL. Breast cancer epithelial-to-mesenchymal transition: examining the functional consequences of plasticity. Breast Cancer Res 2011; 13: 226. [PubMed: 22078097]
32. Fischer KR, Durrans A, Lee S, Sheng J, Li F, Wong ST et al. Epithelial-to-mesenchymal transition is not required for lung metastasis but contributes to chemoresistance. Nature 2015; 527: 472–476. [PubMed: 26560033]
33. Zheng X, Carstens JL, Kim J, Scheible M, Kaye J, Sugimoto H et al. Epithelial-to-mesenchymal transition is dispensable for metastasis but induces chemoresistance in pancreatic cancer. Nature 2015; 527: 525–530. [PubMed: 26560028]
34. Micalizzi DS, Christensen KL, Jedlicka P, Coletta RD, Baron AE, Harrell JC et al. The Six1 homeoprotein induces human mammary carcinoma cells to undergo epithelial-mesenchymal transition and metastasis in mice through increasing TGF-beta signaling. J Clin Invest 2009; 119: 2678–2690. [PubMed: 19726885]
35. Liu Q, Li A, Tian Y, Liu Y, Li T, Zhang C et al. The expression profile and clinic significance of the SIX family in non-small cell lung cancer. J Hematol Oncol 2016; 9: 119. [PubMed: 27821176]
36. Towers CG, Guarnieri AL, Micalizzi DS, Harrell JC, Gillen AE, Kim J et al. The Six1 oncoprotein downregulates p53 via concomitant regulation of RPL26 and microRNA-27a-3p. Nat Commun 2015; 6: 10077. [PubMed: 26687066]

37. Ford HL, Kabingu EN, Bump EA, Mutter GL, Pardee AB. Abrogation of the G2 cell cycle checkpoint associated with overexpression of HSIX1: a possible mechanism of breast carcinogenesis. Proc Natl Acad Sci U S A 1998; 95: 12608–12613. [PubMed: 9770533]
38. Joukov V, Pajusola K, Kaipainen A, Chilov D, Lahtinen I, Kukk E et al. A novel vascular endothelial growth factor, VEGF-C, is a ligand for the Flt4 (VEGFR-3) and KDR (VEGFR-2) receptor tyrosine kinases. EMBO J 1996; 15: 1751. [PubMed: 8612600]
39. Cao Y, Linden P, Farnebo J, Cao R, Eriksson A, Kumar V et al. Vascular endothelial growth factor C induces angiogenesis in vivo. Proc Natl Acad Sci U S A 1998; 95: 14389–14394. [PubMed: 9826710]
40. Skobe M, Hawighorst T, Jackson DG, Prevo R, Janes L, Velasco P et al. Induction of tumor lymphangiogenesis by VEGF-C promotes breast cancer metastasis. Nat Med 2001; 7: 192–198. [PubMed: 11175850]
41. Lund AW, Duraes FV, Hirosue S, Raghavan VR, Nembrini C, Thomas SN et al. VEGF-C promotes immune tolerance in B16 melanomas and cross-presentation of tumor antigen by lymph node lymphatics. Cell Rep 2012; 1: 191–199. [PubMed: 22832193]
42. Yeh YW, Cheng CC, Yang ST, Tseng CF, Chang TY, Tsai SY et al. Targeting the VEGF-C/VEGFR3 axis suppresses Slug-mediated cancer metastasis and stemness via inhibition of KRAS/YAP1 signaling. Oncotarget 2017; 8: 5603–5618. [PubMed: 27901498]
43. Dias S, Choy M, Alitalo K, Rafii S. Vascular endothelial growth factor (VEGF)-C signaling through FLT-4 (VEGFR-3) mediates leukemic cell proliferation, survival, and resistance to chemotherapy. Blood 2002; 99: 2179–2184. [PubMed: 11877295]
44. Su JL, Yen CJ, Chen PS, Chuang SE, Hong CC, Kuo IH et al. The role of the VEGF-C/VEGFR-3 axis in cancer progression. Br J Cancer 2007; 96: 541–545. [PubMed: 17164762]
45. Kampen KR, Scherpen FJG, Mahmud H, Ter Elst A, Mulder AB, Guryev V et al. VEGFC Antibody Therapy Drives Differentiation of AML. Cancer Res 2018; 78: 5940–5948. [PubMed: 30185550]
46. Lin J, Lalani AS, Harding TC, Gonzalez M, Wu WW, Luan B et al. Inhibition of lymphogenous metastasis using adeno-associated virus-mediated gene transfer of a soluble VEGFR-3 decoy receptor. Cancer Res 2005; 65: 6901–6909. [PubMed: 16061674]
47. Zhang D, Li B, Shi J, Zhao L, Zhang X, Wang C et al. Suppression of tumor growth and metastasis by simultaneously blocking vascular endothelial growth factor (VEGF)-A and VEGF-C with a receptor-immunoglobulin fusion protein. Cancer Res 2010; 70: 2495–2503. [PubMed: 20197464]
48. Wang CA, Tsai SJ. The non-canonical role of vascular endothelial growth factor-C axis in cancer progression. Exp Biol Med (Maywood) 2015; 240: 718–724. [PubMed: 25888649]
49. Pinskey JM, Franks NE, McMellen AN, Giger RJ, Allen BL. Neuropilin-1 promotes Hedgehog signaling through a novel cytoplasmic motif. J Biol Chem 2017; 292: 15192–15204. [PubMed: 28667171]
50. Apte RS, Chen DS, Ferrara N. VEGF in Signaling and Disease: Beyond Discovery and Development. Cell 2019; 176: 1248–1264. [PubMed: 30849371]
51. Jimeno A, Weiss GJ, Miller WH Jr., Gettinger S, Eigl BJ, Chang AL et al. Phase I study of the Hedgehog pathway inhibitor IPI-926 in adult patients with solid tumors. Clin Cancer Res 2013; 19: 2766–2774. [PubMed: 23575478]
52. Takebe N, Miele L, Harris PJ, Jeong W, Bando H, Kahn M et al. Targeting Notch, Hedgehog, and Wnt pathways in cancer stem cells: clinical update. Nat Rev Clin Oncol 2015; 12: 445–464. [PubMed: 25850553]
53. Amakye D, Jagani Z, Dorsch M. Unraveling the therapeutic potential of the Hedgehog pathway in cancer. Nat Med 2013; 19: 1410–1422. [PubMed: 24202394]
54. Timoshenko AV, Rastogi S, Lala PK. Migration-promoting role of VEGF-C and VEGF-C binding receptors in human breast cancer cells. Br J Cancer 2007; 97: 1090–1098. [PubMed: 17912247]
55. Wei W, Tweardy DJ, Zhang M, Zhang X, Landua J, Petrovic I et al. STAT3 signaling is activated preferentially in tumor-initiating cells in claudin-low models of human breast cancer. Stem Cells 2014; 32: 2571–2582. [PubMed: 24891218]

56. Vartuli RL, Zhou H, Zhang L, Powers RK, Klarquist J, Rudra P et al. Eya3 promotes breast tumor-associated immune suppression via threonine phosphatase-mediated PD-L1 upregulation. J Clin Invest 2018; 128: 2535–2550. [PubMed: 29757193]

57. Wei T, Simko V. R package “corrplot”: Visualization of a Correlation Matrix (Version 0.84), 2017.

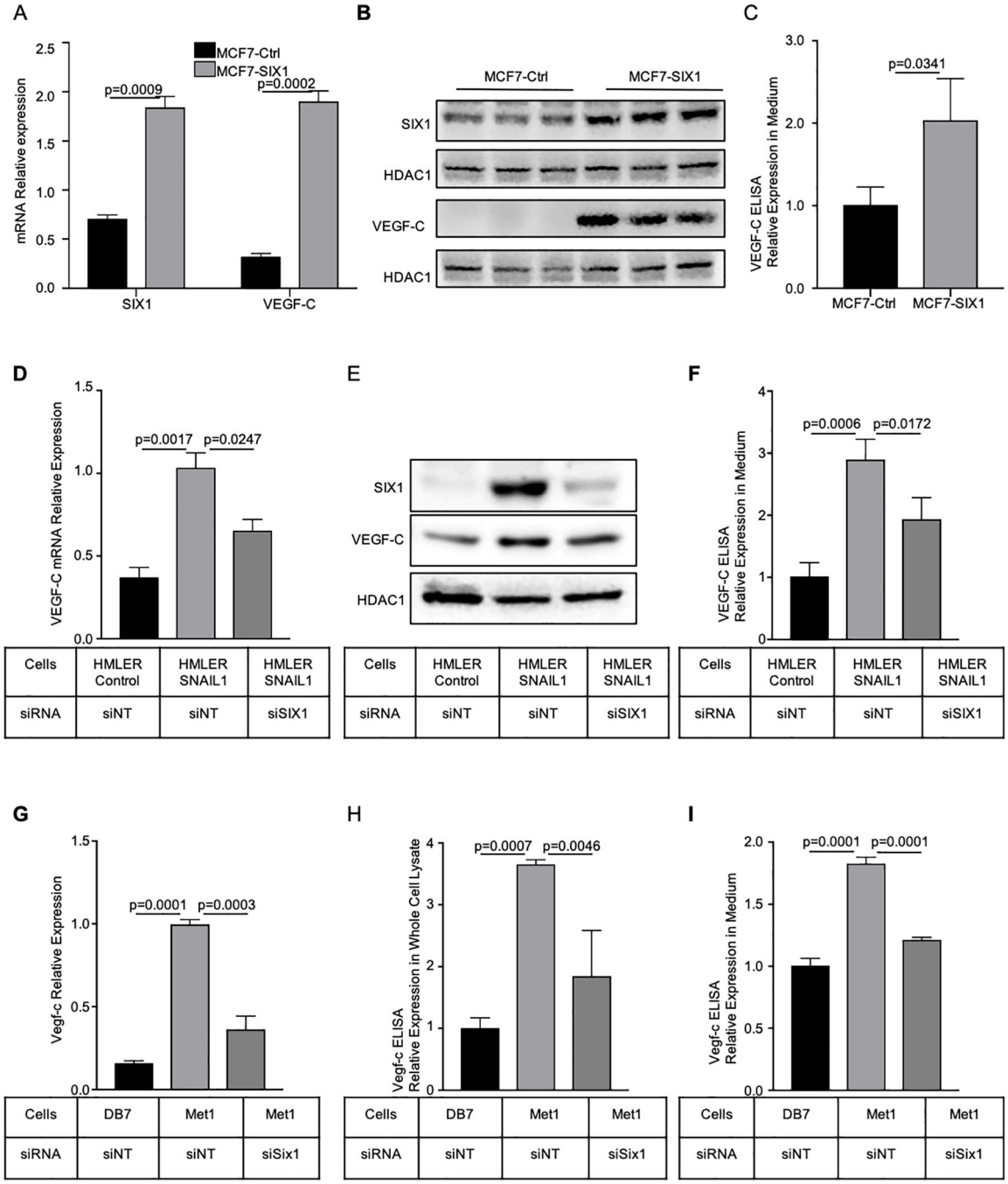

Figure 1.

VEGF-C is downstream of SIX1 in three different models of EMT. (A) qRT-PCR analyses of SIX1 and VEGF-C using 1ug RNA from MCF7-Ctrl and MCF7-SIX1 cells. Gene expression is normalized to α-TUBLIN mRNA. (B) Representative Western blot analysis of whole cell lysates from MCF7-Ctrl and MCF7-SIX1 cells, each sample was run in triplicate. (C) ELISA for VEGF-C performed on 100ul CM taken from the same number of plated MCF7-Ctrl and MCF7-SIX1 cells. (D) VEGF-C qRT-PCR analyses performed on 1ug RNA from HMLER-GFP-siNT, HMLER-SNAILl-siNT and HMLER-SNAIL1-siSIX1 cells. Gene

expression is normalized to α- TUBLIN mRNA. (E) Representative Western blot analysis to examine levels of SIX1 and VEGF-C in whole cell lysates from HMLER-GFP-siNT, HMLER-SNAIL-siNT and HMLER-SNAIL-siSIX1 cells. HDAC was used as a loading control. (F) ELISA for VEGF-C performed on 100ul CM taken from same number of plated HMLER-GFP-siNT, HMLER-SNAIL1-siNT and HMLER-SNAIL1-siSIX1 cells. (G) Vefg-C qRT-PCR analyses performed using 1ug RNA from DB7-siNT, Met1-siNT and Met1-siSix1 cells. Gene expression was normalized to 18s rRNA. (H) Vegf-c ELISA performed on whole cell lysates (40ug protein) from DB7-siNT, Met1-siNT and Met1-siSix1 cells. The experiment was performed two independent times in triplicate, and a representative experiment is shown. (I) Vegf-c ELISA using 100ul CM taken from same number of plated DB7-siNT, Met1-siNT and Met1-siSix1 cells. All experiments in this figure were performed two independent times in triplicate, and representative experiments are shown.

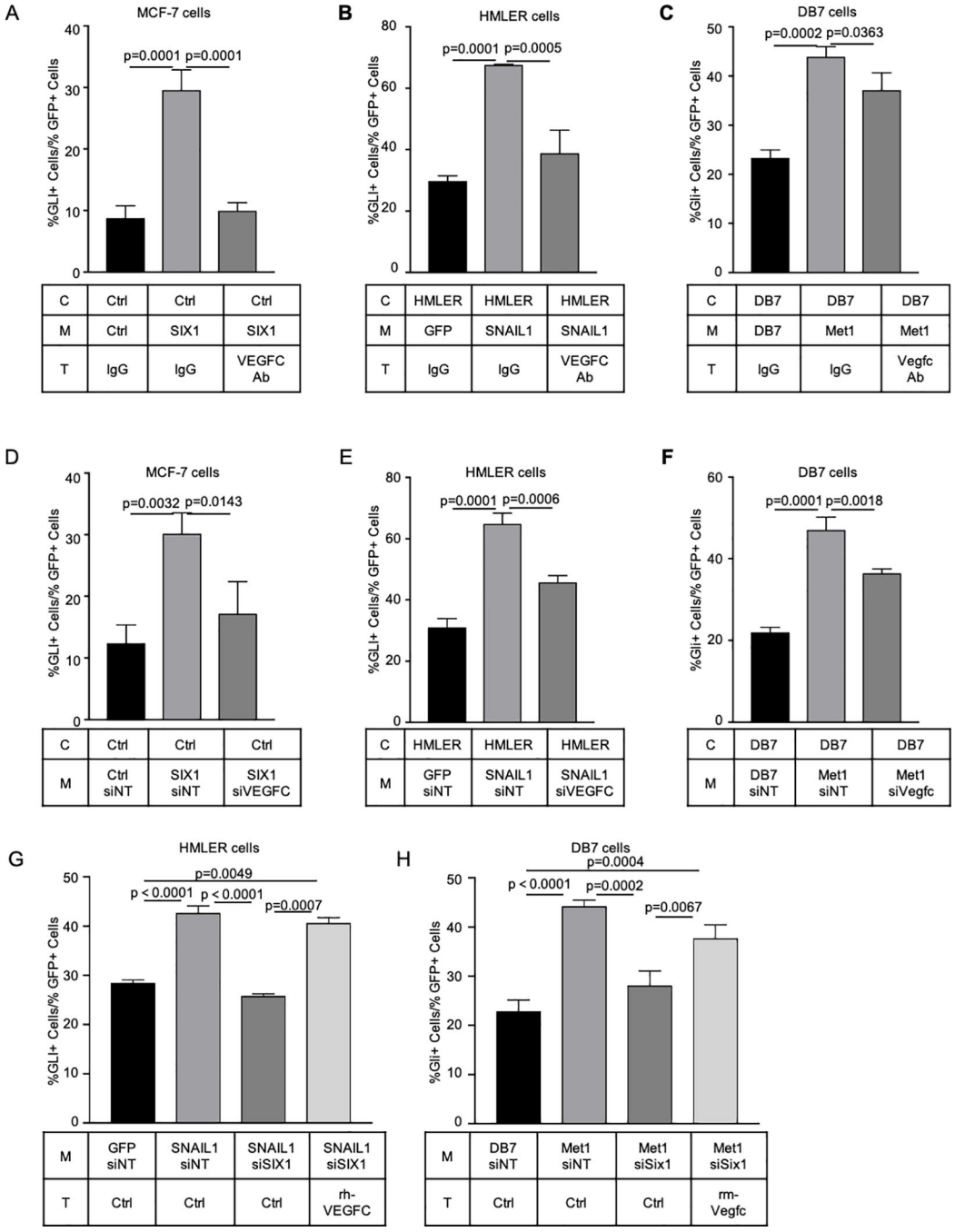

Figure 2.

GLI signaling is activated downstream of VEGF-C. (A, B and C) 7x-GLI promoter GFP reporter assays performed on MCF7-Ctrl, HMLER and DB7 cells, respectively, treated with indicated CM for 48 hours with/without 5 ug/ml VEGF-C antibody (sc-374628) or an equal amount of IgG. (D, E and F) 7x-GLI promoter GFP reporter assays performed on MCF7-Ctrl, HMLER and DB7 cells, respectively, treated for 48 hours with indicated CM taken from EMT cells +/− inhibition of VEGF-C via siRNA (G) GLI reporter assays performed on HMLER cells treated for 48 hours in indicated CM with/without the addition of 100ng/ml

recombinant human VEGF-C. (H) Gli reporter assays performed on DB7 cells treated for 48 hours in indicated CM with/without the addition of 100ng/ml recombinant mouse Vegf-c. All experiments shown in this figure were performed twice in triplicate, and a representative experiment is shown.

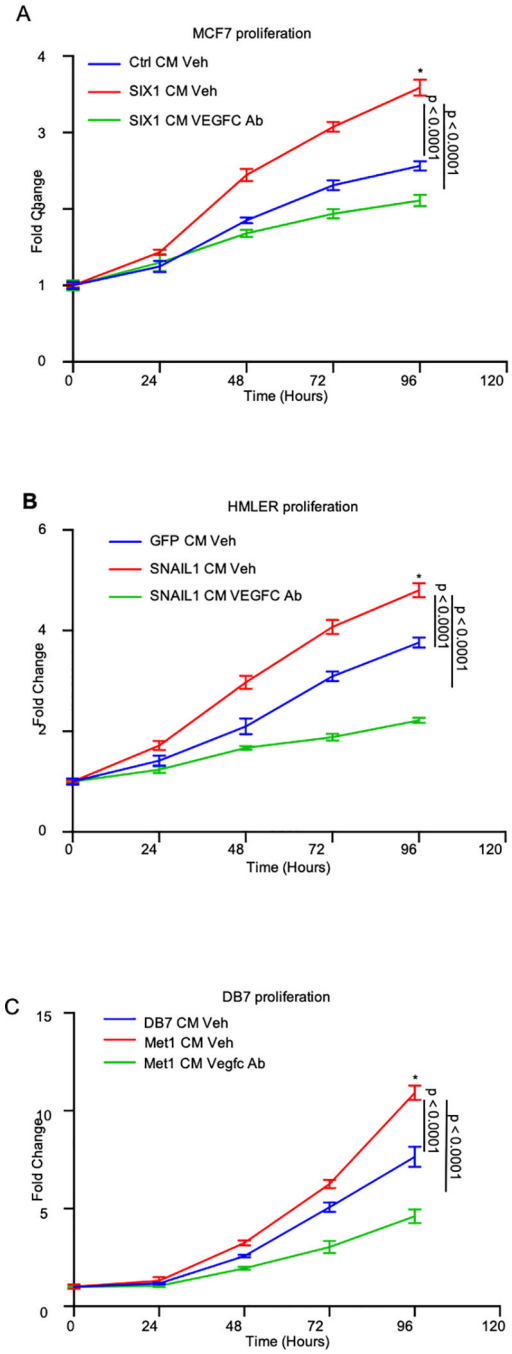

Figure 3.

VEGF-C, secreted by EMT cells, leads to increased growth of epithelial cancer cells. (A) Cell growth assessed using CellTiter-Glo for MCF7-Ctrl cells grown for 96 hours in indicated CM with/without 5 ug/ml of the neutralizing VEGF-C antibody (sc-374628) or an equal amount of IgG. (B) Same as in panel A but performed on HMLER-GFP cells in indicated CM. (C) Same as in panel A but performed on DB7 cells in indicated CM. Cell growth experiments were performed two independent times with 5 replicates for each time point, and a representative experiment is shown.

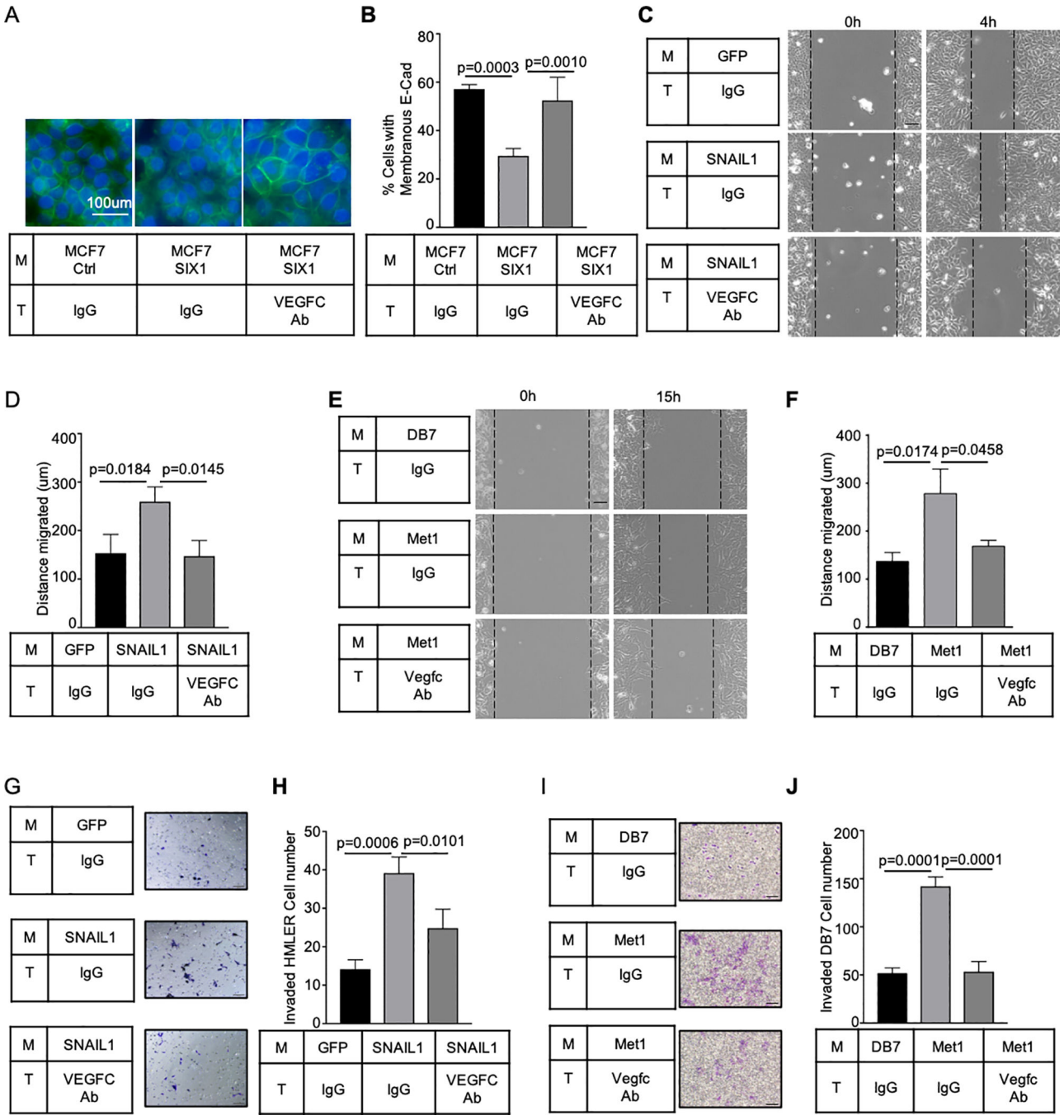

Figure 4.

EMT cell-induced VEGF-C mediates aggressive phenotypes in epithelial cancer cells. (A) Representative ICC of E-cadherin (green) performed on MCF7-Ctrl cells grown for 48 hours in indicated CM with/without 5ug/ml VEGF-C antibody (sc-374628) or an equal amount of IgG. Dapi (blue), scale bar is 100μm. (B) Quantitation of % membranous E-cadherin in panel A, the experiments were performed two independent times, 5 fields (200x magnification) per condition were counted for each experiment and a representative experiment is shown. (C) Representative migration assay (4–6 hours) performed on

HMLER-GFP cells in indicated CM with/without 5ug/ml VEGF-C antibody (sc-374628) or an equal amount of IgG. Scale bar is 100um. (D) Quantitation of cell migration in panel C. (E and F) Same as panel C and D but performed on DB7 cells in indicated CM, and cells were allowed to migrate for 15h. Migration experiments were performed two independent times in triplicate wells. 2 fields (100x magnification) per well were quantified and a representative experiment is shown. (G) Representative invasion assay performed on HMLER-GFP cells grown in indicated CM for 24h with/without 5ug/ml VEGF-C antibody (sc-374628) or an equal amount of IgG. Scale bar is 100um. (H) Quantitation of cell invasion in panel G. (I and J) Same as panel G and H but performed on DB7 cells grown in indicated CM for 24h. Invasion experiments were performed two independent times, each in 5 replicate wells, 1 field (200x magnification) per well was quantified and a representative experiment is shown.

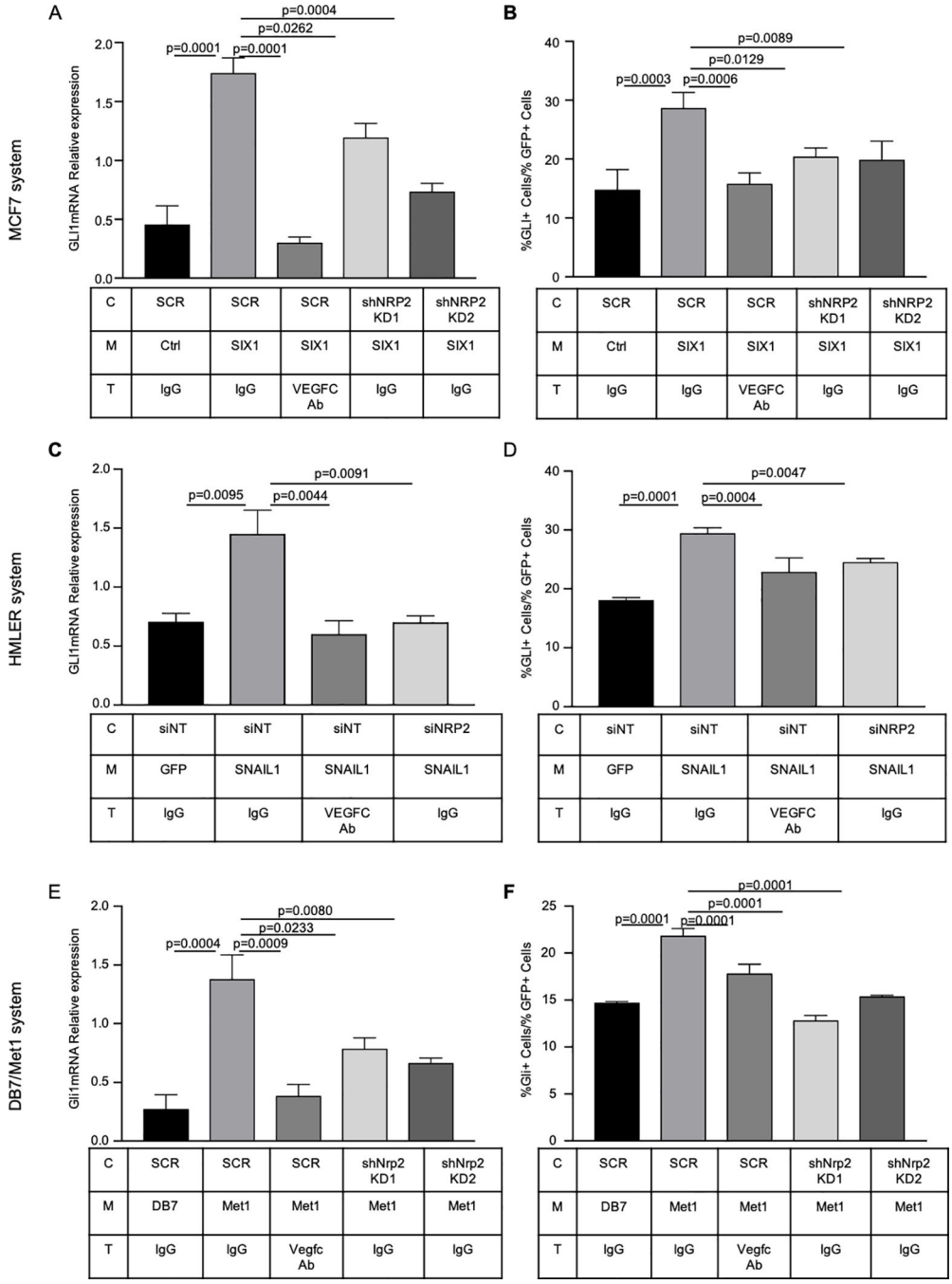

Figure 5.

NRP2 expressed on epithelial cancer cells is necessary for VEGF-C to activate GLI signaling. (A) GLI1 qRT-PCR analyses performed on 1ug RNA from MCF7-Ctrl-SCR and MCF7-Ctrl-shNRP2 cells treated for 48 hours in indicated CM with/without 5ug/ml VEGF-C antibody (sc-374628) or an equal amount of IgG. Gene expression is normalized to α-TUBLIN mRNA. (B) GLI reporter analyses performed on MCF7-Ctrl-SCR and MCF7-Ctrl-shNRP2 cells grown for 48 hours in indicated CM with/without 5ug/ml VEGF-C antibody (sc-374628) or an equal amount of IgG. (C) GLI1 qRT-PCR analyses performed on 1ug

RNA from HMLER-siNT and HMLER-siNRP2 cells grown for 48 hours in indicated CM with/without 5ug/ml VEGF-C antibody (sc-374628) or an equal amount of IgG. Gene expression is normalized to α-TUBLIN mRNA. (D) GLI reporter analyses performed on HMLER-siNT and HMLER-siNRP2 cells grown for 48 hours in indicated CM with/without 5ug/ml VEGF-C antibody (sc-374628) or an equal amount of IgG. (E) Gli1 qRT-PCR analyses performed on 1ug RNA from DB7-SCR and DB7-shNrp2 cells grown for 48 hours in indicated CM with/without 5ug/ml Vegf-c antibody (sc-374628) or an equal amount of IgG. Gene expression is normalized to 18s rRNA. (F) 7x-Gli promoter GFP reporter analyses performed on DB7-SCR and DB7-shNrp2 cells grown for 48 hours in indicated CM with/without 5ug/ml Vegf-c antibody (sc-374628) or an equal amount of IgG. All experiments (qRT-PCR and Gli reporter assays) within this figure were performed at least two independent times in triplicate, and a representative experiment for each panel is shown.

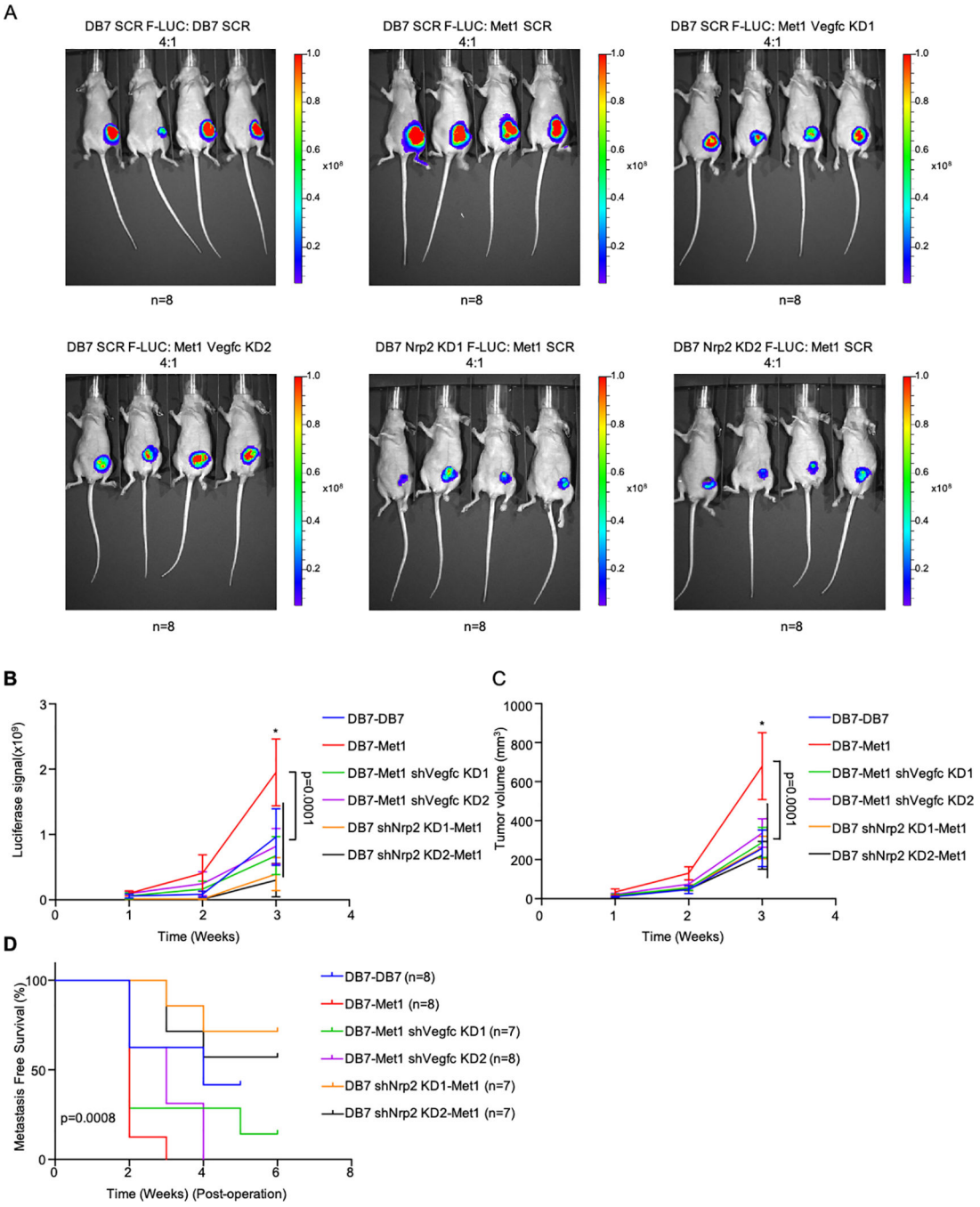

Figure 6.

Vegf-c KD in Met1 (EMT) cells or Nrp2 KD in epithelial DB7 mammary carcinoma cells can inhibit Met1 induced growth and metastasis of DB7 cells *in vivo*. (A) Representative luminescent images of nude mice taken at the same time point (three weeks after injection of cells). (B) Quantitation of luminescent signal (representing DB7 cells) in primary tumors in indicated mixed tumors groups. (C) Quantitation of primary tumor volume in indicated mixed tumors groups, as measured using calipers (thus representating total tumor volume

including both DB7 and Met1 cells). (D) Kaplan Meier curve for metastasis-free-survival in indicated mixed tumors groups.

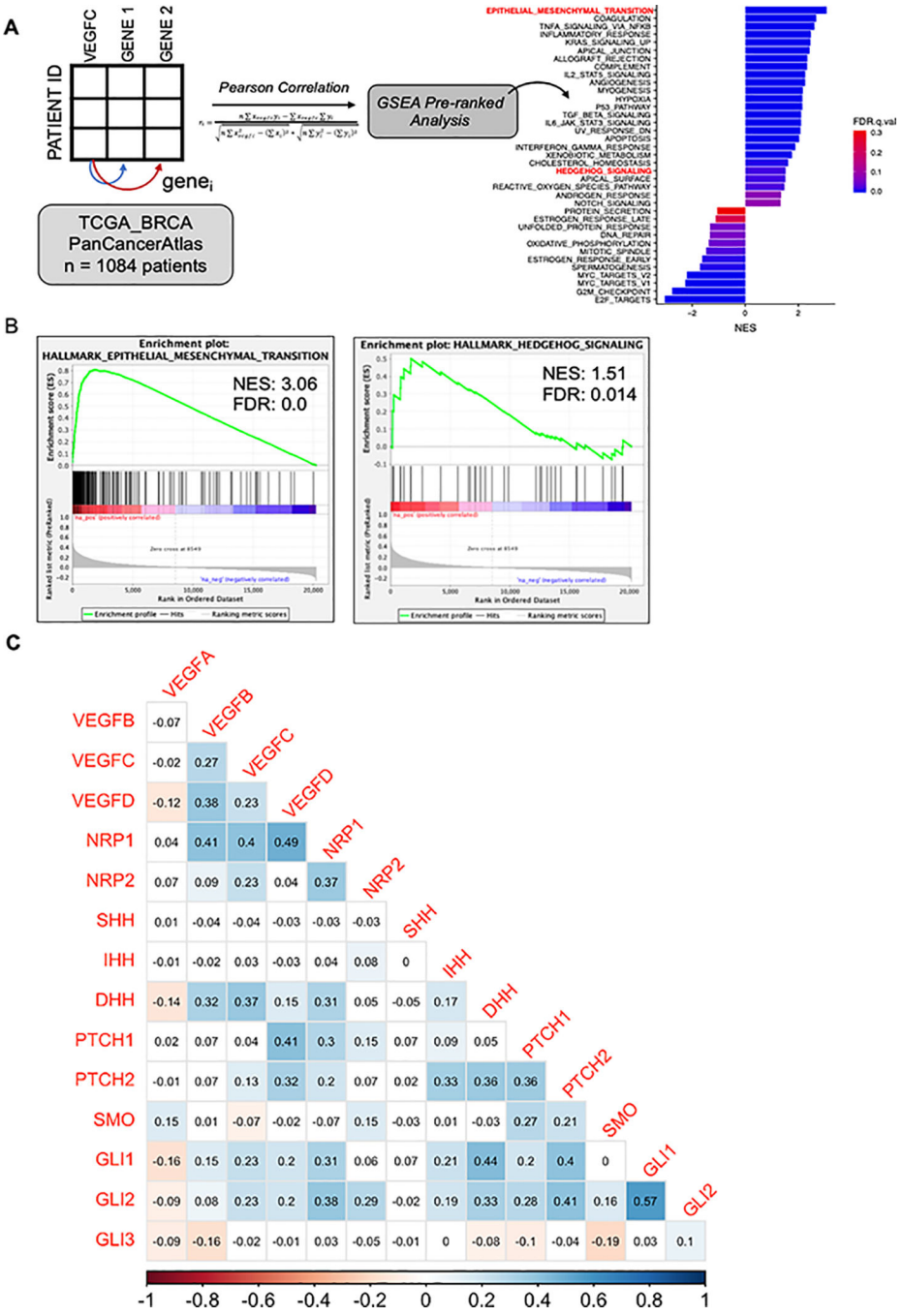

Figure 7.

VEGFC positively correlates with Hh pathway genes in human breast tumors. (A) Pairwise gene correlates with VEGFC are enriched for EMT and Hedgehog pathways. (Left schematic) Pearson correlations performed across all genes against VEGFC were ranked and analyzed by GSEA. (Right panel) Top significantly enriched pathways correlated with VEGFC expression plotted by Normalized Enrichment Score (NES) and FDR. Among the top enriched pathways were the EMT and Hedgehog Signaling pathways. (B) GSEA enrichment plots for the EMT and Hedgehog gene signatures. Red hits represent genes most

strongly correlated with VEGFC expression and blue hits genes weakly correlated with VEGFC expression. (C) The R package `corrplot` [57] (ref: Taiyun Wei and Viliam Simko (2017). R package "corrplot": Visualization of a Correlation Matrix (Version 0.84), Available from https://github.com/taiyun/corrplot) was used to plot Pearson correlation coefficients and p-values. All significant correlation values (i.e. those with p-value ≤ 0.01) were plotted on a −1 (red) to 0 (white) to blue (1) color scale while pairs with statistically non-significant correlations were plotted without colors. Triangle plots were created to reduce data redundancy and crowding.

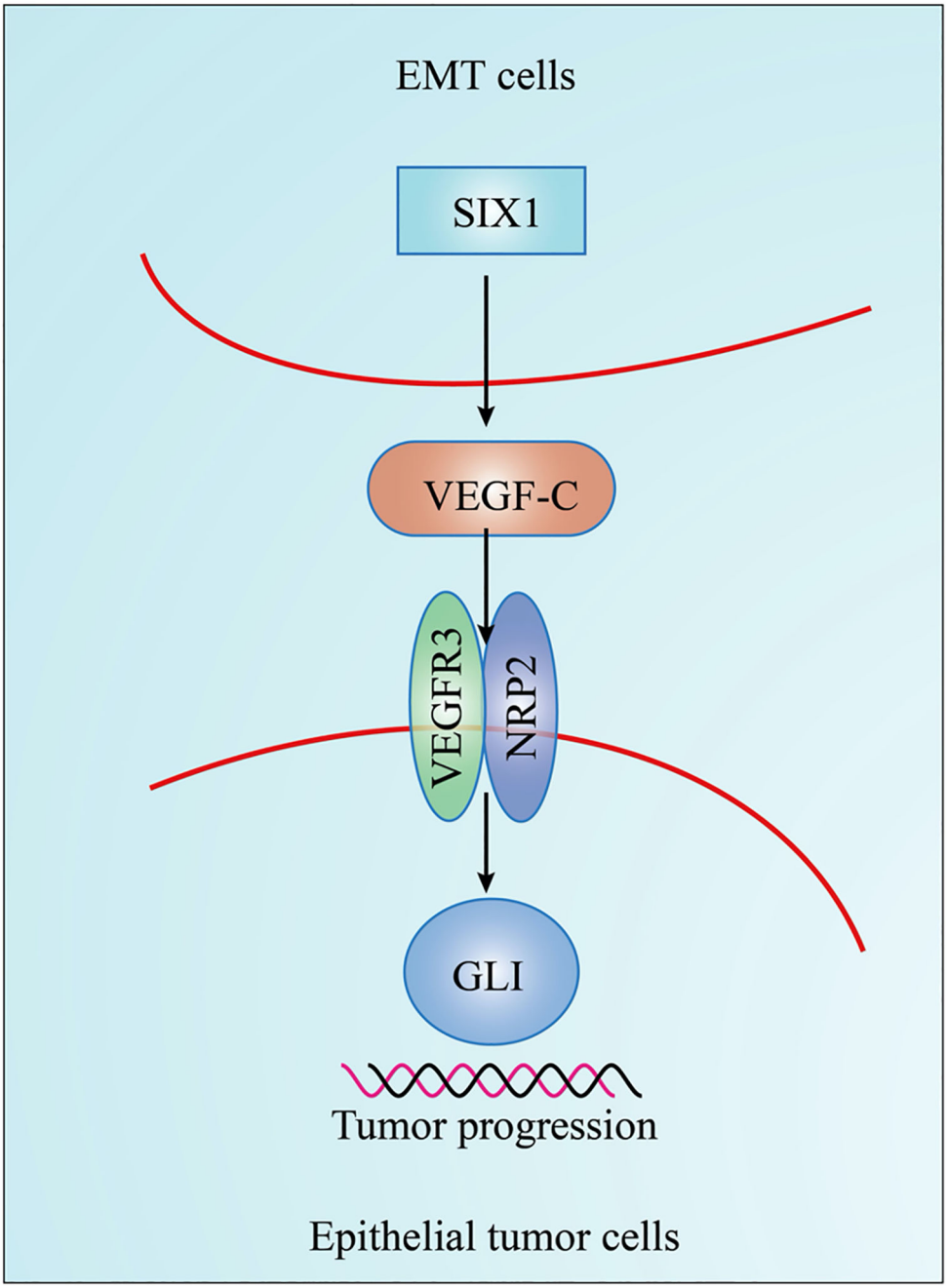

Figure 8.

Model to demonstrate how SIX1, when expressed in cells that display characteristics of EMT, induces VEGF-C, which is secreted from the EMT cells and activates GLI signaling via NRP2/FLT4 in neighboring epithelial tumor cells, ultimately, promoting tumor progression.